ISSN 0030-400X, Optics and Spectroscopy, 2009, Vol. 107, No. 5, pp. 796–802. © Pleiades Publishing, Ltd., 2009.
Original Russian Text © L.A. Ageev, K.S. Beloshenko, E.D. Makovetsky, V.K. Miloslavsky, 2009, published in Optika i Spektroskopiya, 2009, Vol. 107, No. 5, pp. 838–745.

PHYSICAL OPTICS

Implantation of Periodic Structures Formed by Silver Particles into Quartz Glass

L. A. Ageev, K. S. Beloshenko, E. D. Makovetsky, and V. K. Miloslavsky

Karazin Kharkov National University, Kharkov, 61077 Ukraine

e-mail: Leonid.A.Ageev@univer.kharkov.ua

Received April 23, 2009

Abstract—Quartz glass samples with a thin photosensitive AgCl–Ag film, prepared by successive evaporation of AgCl ($h_{AgCl} \approx 35$ nm) and Ag ($h_{Ag} \approx 8$ nm) in vacuum have been investigated. A periodic structure with a period of $d = 375$ nm formed by Ag particles was obtained in films using a *p*-polarized laser beam ($\lambda = 532$ nm, $P = 25$ mW) at an angle of incidence of $\varphi = 20°$. After removing AgCl in a fixing agent, the periodic structure remained on the glass surface. Subsequent irradiation by a CO_2 laser ($\lambda = 10.6$ μm, $P \approx 20$ W) led to the implantation of this structure into the glass with the conservation of its period *d* and partial conservation of the related dichroism. The fact of implantation is confirmed by the high mechanical and chemical stability of the structure obtained. A possible implantation mechanism, taking into account the thermionic emission, Ag ionic transport, and the presence of free voids in the quartz glass and defects in its structural network, is discussed.

PACS numbers: 78.20.Ci

DOI: 10.1134/S0030400X09110186

INTRODUCTION

Coloring of dielectrics by very small metal particles has been known for long. However, this problem remains urgent in view of the developing optics of nanostructures and nonlinear optics [1, 2]. The studies published approximately before 1995 and devoted to the optics of metal clusters were reviewed in monograph [2]. In particular, it was noted in [2] that it is fairly difficult to incorporate clusters into optical quartz glass and only one method was described for this purpose, i.e., joint vacuum deposition of metal and quartz [3]. Ion implantation and the sol–gel technique were applied later [4, 5] to incorporate Ag into quartz glass. The method of chemical incorporation of particles into specially prepared mesoporous quartz is also known [6].

Along with the implantation problem, the modification of implanted metal nanoparticles in dielectrics under laser irradiation [7] is also of interest. The irradiation of Ar^+-doped silicate glass by an Ag^+ laser was investigated in [8]. It was shown that this treatment leads to the formation of Ag particle chains on the glass surface, which produces weak dichroism. Ag-containing SiO_2 films were prepared in [9] by magnetron sputtering on a glass substrate. Ag nanostructurization in a film, which leads to the formation of a plasma absorption band, was obtained by sample annealing or combining annealing with laser irradiation (Nd-laser harmonic). It was found that the irradiation by a *p*-polarized beam with $\lambda = 532$ nm leads to the formation of a periodic surface relief with a period close to $\approx\lambda$.

In addition, thermally induced implantation of isotropic colloidal Ag into optical quartz glass was recently realized by irradiating a thin island Ag film on the glass surface by a cw CO_2 laser ($\lambda = 10.6$ μm, $P \approx 30$ W) [10, 11]. In this study, we continue the aforementioned investigations and show the possibility of implanting anisotropic (periodic) silver structures into quartz glass; these structures are photoinduced in a photosensitive AgCl–Ag film on quartz surface.

EXPERIMENTAL

The experiment was performed with approximately 1.5–2-μm-thick KU quartz glass plates. An AgCl film with a thickness of $h \approx 35$ nm was thermally deposited on the plate in vacuum with the subsequent deposition of an island Ag film less than 10 nm thick. The AgCl–Ag film was photosensitive to visible light. The irradiation of the film by a linearly polarized cw laser beam induces periodic structures (PSs) in it related to the film waveguide properties [12–14].

A PS is formed under single-beam irradiation. In our experiment, a prepared sample was irradiated by a *p*-polarized cw laser beam ($\lambda = 532$ nm, $P \approx 25$ mW) at an angle of incidence of $\varphi = 20°$. The PS period *d* depends on λ and φ.

The investigations were carried out on irradiated film portions with an area of about 10 mm^2. This size is determined by the laser beam cross section. The

exposure time that is necessary to form a PS depends on the beam intensity (W/cm^2); at the above-mentioned power it was ~10 min. In this case, the PS is developed to saturation.

The PSs formed in the AgCl–Ag film were fixed by dissolving AgCl in a fixing agent (hyposulfite solution) [13]. After fixing, rinsing in water, and drying, the silver-based PS remained on the substrate. Then the PS-containing areas were irradiated with a cw-CO_2-laser beam ($\lambda = 10.6$ μm). At a beam power of $P \approx 20$ W and exposure time of about 1 min, the irradiated portion was heated so as to obtain silver film luminescence close to white, after which the irradiation stopped. After irradiation, the silver was removed from the quartz surface by wiping it with a soft, clean, wet tissue, then with a dry one. After this procedure, a spot remained in the irradiated area, which was yellow in transmitted white light. This is a sign of silver implanted in the quartz glass surface layer (this color is characteristic of colloidal Ag particles). The silver penetration into quartz was confirmed by the high durability of the irradiated region against not only wiping with tissue but also rougher mechanical treatments (for example, scratching with a sewing needle). The chemical stability of this region was also high: an arbitrarily long exposure to saturated vapor iodine does not lead to Ag transformation into transparent AgI, whereas the silver on the substrate surface was completely iodinated. However, exposure of the sample to 50% solution of sulfuric acid led to the almost complete removal of the implanted silver (only small regions remained, which were stable to this effect). These regions retained the light diffraction, which is characteristic of the PSs formed by Ag particles. The regions with dissolved silver exhibited a weaker diffraction, which was related to the periodic quartz deformation, retaining the memory of PS after Ag removal. Note that, in contrast to the PS implantation under consideration, the fine-grained isotropic Ag colloid implanted into quartz glass is stable to acid [10, 11].

The PS periods and structures were investigated using diffractometry and microscopy. The diffraction measurements were based on laser beam diffraction ($\lambda = 532$ nm) from a PS in reflection, according to the autocollimating scheme [13]. The quartz surface structure was studied with an atomic force microscope, and a transmission electron microscope (TEM) was used to analyze the PS on the surface of auxiliary samples prepared on conventional (K-8) glass.

In all stages, beginning with the preparation of AgCl–Ag film and including PS implantation into quartz glass, the optical density spectra were measured in polarized light using an SF-26 spectrophotometer adapted for these measurements.

RESULTS

PSs are known to form in AgCl–Ag films due to the transport of silver to interference minima [12, 13]. The interference arises upon the interaction of an incident beam with the TE_0 waveguide mode scattered in the film. At the aforementioned AgCl film thickness and development of the PS to saturation, the effective refractive index of this mode is equal to the quartz substrate refractive index $n_c = 1.46$. The PS period d under a p-polarized beam is given by the formula

$$d = \lambda/\sqrt{n_c^2 - \sin^2\varphi}. \quad (1)$$

At $\lambda = 532$ nm and $\varphi = 20°$, formula (1) yields $d = 375$ nm. These conditions are chosen because the PSs formed by a p-polarized beam are closest to perfect diffraction gratings [12, 13].

After the PS formation and sample fixing, we measured the period d. During the measurements, a laser beam passed through a screen with a hole and was incident on the PS at the angle at which the diffracted beam of the first diffraction order in reflection reached the screen (Fig. 1a). The general view of the beam in the screen indicates that the PS is imperfect in comparison with an ideal diffraction grating. The maximum brightness is concentrated in the small region *4* of intersection of two symmetric, relatively weak arc-shaped bands. However, the area of region *4* (characterized by maximum brightness) differs only slightly from the cross-sectional area of the measuring laser beam *3* incident on the PS. This concentration of brightness indicates that the PS-forming lines are essentially linear and parallel. At the same time, the presence of bands in the diffraction pattern indicates the existence of deviations from strict linearity and parallelity. The PS period was determined by measuring the autocollimation angle φ_a, at which the point of maximum brightness in the diffraction pattern lies on the axis of the incident laser beam *1*. In this case,

$$d = \lambda/2\sin\varphi_a. \quad (2)$$

The measured d values coincided with the d value calculated from (1) with a deviation of no more than ±0.5 nm.

The PS structure was investigated by TEM on an auxiliary sample: K-8 glass (8 ($n_c = 1.52$) with the same AgCl–Ag film as on quartz. To obtain approximately the same period as on quartz, the angle of incidence of the laser beam was chosen to be $\varphi = 30°$. The calculation from formula (1) and measurement after fixing gave $d = 371$ nm. The sample was prepared for TEM analysis as follows: it was fixed and a thin carbon film was deposited on it, with subsequent separation of this film with a PS from the substrate using gelatin, gelatin dissolution on the surface of heated water, and the extraction of the carbon film with PS from water to be placed on the TEM grid. The general view of the PS on an area of about 200 μm^2 is shown in Fig. 1b. Since

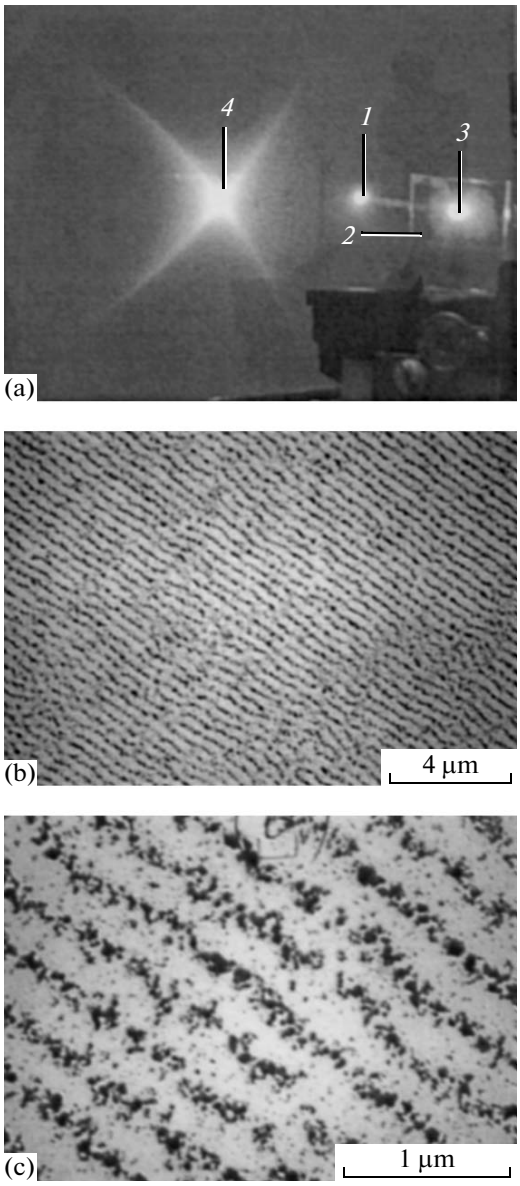

Fig. 1. (a) Diffraction pattern ((*1*) hole in the screen for transmitting a laser beam to the sample (laser is behind the screen), (*2*) sample on a goniometer, (*3*) PS-containing portion exposed to a laser beam, and (*4*) screen image of the beam diffracted into the first order from PS in reflection (the angle of beam incidence on PS is $\varphi = 35°$)) and (b, c) TEM images of PSs with a period $d = 371$ nm formed on K-8 glass.

the PS is developed as a result of the excitation of a TE waveguide mode in the AgCl–Ag film, the PS line direction coincides with the polarization direction $\mathbf{E}_0$ of the inducing laser beam [12, 13]. The line structure is shown in greater detail in Fig. 1c. It can be seen that the PS lines consist of clusters and individual (mainly spherical) Ag particles with an average size of ~10 nm. There are many very small particles (< 10 nm in size) between lines. Figure 1b shows the general view of PS and its deviation from an ideal diffraction grating: one can see that the lines are not strictly linear and parallel. These deviations from ideality determine the diffraction pattern in Fig. 1a.

As was noted above, a PS is implanted into a quartz glass surface layer under CO_2-laser irradiation. After implantation, the quartz surface was analyzed by AFM. The results are shown in Figs. 2a and 2b. The analysis of a surface area of 10×10 μm (Fig. 2a) shows the presence of a periodic surface relief with the same period $d = 375$ nm as the PS prepared on the quartz surface before the implantation. The exact d value is found from the diffraction pattern of the region with the PS implanted into quartz; in this case, the pattern diffraction is nearly the same as in Fig. 1a. The bright and dark areas in the photographs in Figs. 2a and 2b correspond, respectively, to hills and valleys on the quartz surface. The average relief height is about 10 nm. It should be noted that all relief details correspond to deformed quartz surface, whereas silver particles are under this surface and cannot be directly seen in the AFM image.

Figure 2b shows the portion obtained by scanning an area of 3×3 μm. One can see that the surface contains volcano-like aggregates with craters at the center, whose depth (according to the AFM data) may reach 40 nm. The volcano walls rise above the surface by ~10 nm. We believe these formations to be the sites of Ag particle incorporation into the quartz layer surface.

Figure 2c shows a fragment of AFM image of a small 1×1 μm area of clean quartz surface. We intentionally chose a region with pronounced surface defects in the form of round pits several tens of nanometers in diameter. According to the AFM data, their depth is about 40 nm. The pit edges do not rise above the surface. The surface has a relief with an average height of ~1 nm. The density of these defects was not investigated, but they are fairly rare. One might suggest that the pits can be formed as a result of the agglomeration of natural voids inherent in quartz glass [16].

Figure 3 presents the optical density spectra ($D = \ln(T^{-1})$ and T is the transmittance). Curve *1* (Fig. 3a) corresponds to the as-prepared AgCl–Ag film before laser irradiation. The presence of maximum in the range $\lambda \approx 470$–480 nm and a monotonic decrease in $D(\lambda)$ with an increase in λ indicates that the structure of the Ag film deposited on the AgCl surface is intermediate between mosaic and colloidal. The presence of small spherical grains, which form a two-dimensional colloid on the AgCl surface, is evidenced by a D maximum related to the plasma resonance in grains.

It is known that the exposure of an AgCl–Ag film to red light leads to the formation of colloidal particles, which are distributed throughout the polycrystalline AgCl film volume; the plasma resonance band peaks in the range of 500–550 nm in this case, and a spectral hole is formed near the irradiation wavelength

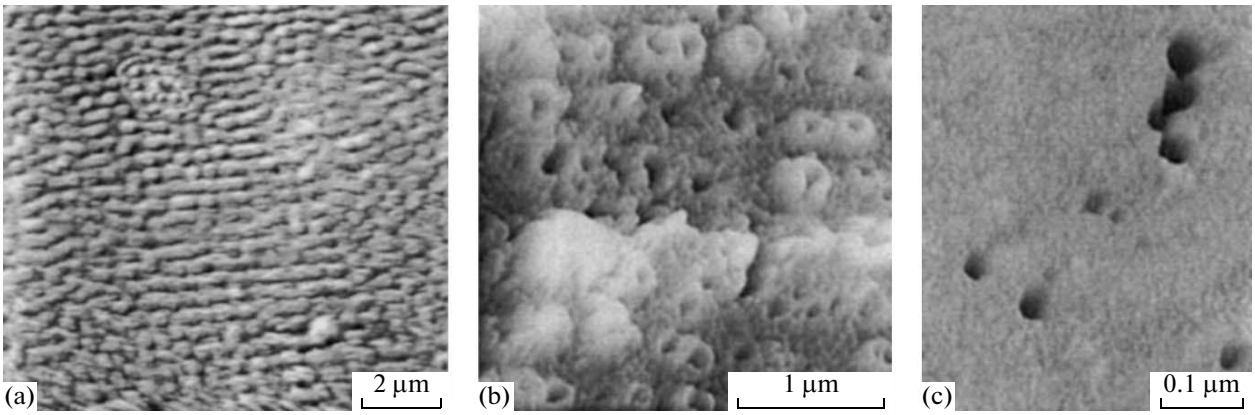

Fig. 2. AFM images of (a, b) quartz glass surface portions with implanted PS ($d = 375$ nm), obtained by scanning areas (a) 100 and (b) 9 μm^2 in size and (c) clean glass surface, obtained by scanning an area 1 μm^2 in size.

[12, 13]. The linearly polarized green ($\lambda = 532$ nm) laser beam, which was used to form the PS, also forms a colloid, but simultaneously burns a polarized spectral hole in the colloid absorption band near its wavelength, which is close to the colloid band peak wavelength in the AgCl–Ag composite system. The optical density spectra (measured in polarized light) are shown in Fig. 3a (curves *2*, *3*). Curve *2* corresponds to the polarization orientation $\mathbf{E} \parallel \mathbf{E}_0$, where $\mathbf{E}$ and $\mathbf{E}_0$ are, respectively, the polarization directions of the measuring and PS-inducing laser beams. Spectrum *3* was measured at $\mathbf{E} \perp \mathbf{E}_0$. The minimum in spectrum *2* corresponds to the polarized hole in absorption near the acting laser beam wavelength. The hole has a dual nature; in the initial stage of exposure, it is developed due to the hole burning in the inhomogeneously broadened colloid absorption band and then, after reaching the threshold exposure of PS formation ($\approx$10 J cm^{-2}), it is amplified due to the silver transport to the interference minima during PS development [13]. The significant difference between spectra *2* and *3* corresponds to the photoinduced linear dichroism (Weigert effect, which has been known for a long time in photography [15]). The maximum dichroism reaches the value $\Delta D = D_\perp - D_\parallel \approx 0.5$.

Spectra *1* ($\mathbf{E} \parallel \mathbf{E}_0$) and *2* ($\mathbf{E} \perp \mathbf{E}_0$) in Fig. 3b were measured after sample fixing. The structure of the PS formed by silver and remaining on the quartz substrate surface after fixing corresponds approximately to that shown in Figs. 1b and 1c. The reasons for the change in the spectra *1* and *2* (Fig. 3b) in comparison with spectra *2* and *3* (Fig. 3a) are as follows. While the sample is fixed, silver is partially washed out from the AgCl film volume during AgCl dissolution in the fixing agent, which leads to a decrease in the optical density and dichroism. The blue shifts of spectral peaks are mainly related to the reduced dielectric constant of the medium around Ag particles.

Finally, spectra *3* ($\mathbf{E} \parallel \mathbf{E}_0$) and *4* ($\mathbf{E} \perp \mathbf{E}_0$) (Fig. 3b) were measured after thermally induced PS implantation into quartz under CO_2-laser irradiation. The quartz surface structure after the implantation is shown in Figs. 2a and 2b. When comparing spectra *1, 2* and *3, 4*, one can see that the implantation leads to a decrease in the optical density, diffusion of spectral peaks, and decrease in dichroism. Note that the implantation occurs at a temperature of $T \sim 1000$–1300°C, which exceeds the Ag melting temperature (960.8°C). Therefore, one would observe a thermally induced transformation of the Ag film structure and related diffusion of the spectra. A more unexpected result is that spectra *3* and *4* retain the main features in comparison with spectra *1* and *2* and that the implanted structure retains periodicity (Fig. 2a).

RESULTS AND DISCUSSION

The structural elements of quartz glass are silicon–oxygen tetrahedra $[SiO_4]^{4-}$ (Fig. 4a) [16–18]. The structural network of quartz glass is formed by tetrahedra with vertices connected via oxygen bridges. The quartz glass spatial framework differs from a geometrically regular grating of crystalline quartz by the absence of long-range order in the position and orientation of tetrahedra (Fig. 4b). The main distortions in the quartz glass structure are related to the variation in the Si–O–Si bond angle α between neighboring tetrahedra and the difference in the positions of oxygen atoms in the circles shown in Fig. 4a. Since neighboring tetrahedra are bound via oxygen atoms, there are voids in the quartz glass structure, which are limited in space by bridge oxygen atoms. Figure 4b shows voids of different sizes in the flat projection that are bounded by rings composed of four to eight tetrahedra. Due to the presence of free voids, quartz glass has the highest gas permeability in comparison with other silicate glasses.

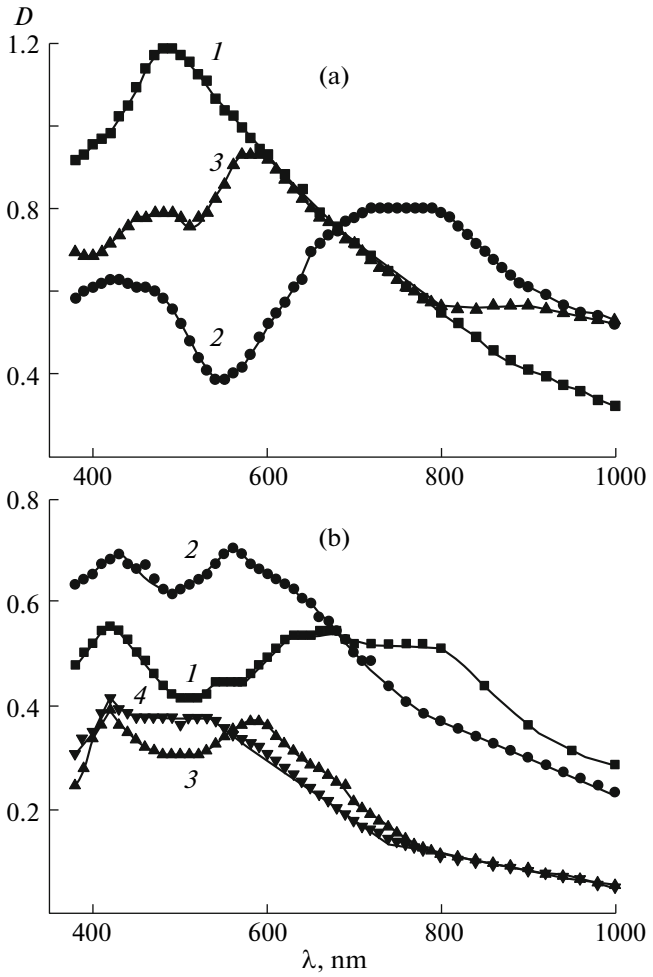

Fig. 3. Optical density spectra of (a) (*1*) the initial quartz glass sample with an AgCl–Ag film on the surface and (*2*, *3*) the sample irradiated with a laser beam ($\lambda = 532$ nm) with a polarization direction $\mathbf{E}_0$ (measurements in polarized light (**E**) at (*2*) $\mathbf{E} \parallel \mathbf{E}_0$ and (*3*) $\mathbf{E} \perp \mathbf{E}_0$) and (b) the sample after fixing (measurements at (*1*) $\mathbf{E} \parallel \mathbf{E}_0$ and (*2*) $\mathbf{E} \perp \mathbf{E}_0$ and after implanting (*3*) $\mathbf{E} \parallel \mathbf{E}_0$ and (*4*) $\mathbf{E} \perp \mathbf{E}_0$).

The voids in quartz glass are responsible for its lower density ($\rho_g = 2.202$ g/cm^3) and refractive index in comparison with crystalline quartz (ρ_k, n_k) ($\rho_c = 2.646$ g/cm^3, $\rho_k = 2.646$ g/cm^3; $n_c = 1.461$, $n_k = 1.551$) [19] (the n values are taken for $\lambda = 0.53$ μm, n_k is the average value for ordinary and extraordinary waves). The possibility of thermally induced implantation of Ag particles under CO_2-laser irradiation should apparently be related to the voids and other structural defects in quartz glass [16].

In the case of implantation of isotropic Ag colloid into quartz glass, we used the model of a medium with the effective permittivity ε_{ef} and analyzed it based on the Maxwell-Garnet (MG) formula [10, 11]. This model should also be valid in the description of pure quartz glass. Based on the assumption that voids in quartz glass have $\varepsilon = 1$, the MG formula can be written as

$$\frac{\varepsilon_{ef} - \varepsilon_k}{\varepsilon_{ef} + 2\varepsilon_k} = q\frac{1 - \varepsilon_k}{1 + 2\varepsilon_k}, \quad (3)$$

where ε_{ef} should coincide with n_c^2, q is the quartz glass void occupancy factor

$$q = NV, \quad (4)$$

N is the void concentration, and V is the void volume. Assuming that the difference in the densities of crystalline quartz and glass is due to the presence of voids in quartz glass, one can find q using the relation

$$\rho_c/\rho_k = 1 - q.$$

The above-mentioned ρ values yield $q = 0.168$. Now, one can calculate the quartz glass refractive index from (3) as follows:

$$\varepsilon_{ef} = n_c^2 = \frac{\varepsilon_k[1 + 2\varepsilon_k - 2q(\varepsilon_k - 1)]}{1 + 2\varepsilon_k + q(\varepsilon_k - 1)}. \quad (5)$$

The calculation according to (5) yields $n_c = 1.457 \approx 1.46$, which, with an accuracy of two decimal places, coincides with the tabular value of n_g. This result indicates that the MG model is valid for a comparative description of crystalline quartz and quartz glass.

It was suggested in [10, 11] that the implantation of Ag particles is related to the thermal diffusion of electrons and Ag^+ in quartz glass. The electron traps in quartz glass are void walls. Ag^+ ions recombine with trapped electrons to form Ag atoms in voids, which in turn become traps for electrons. As a result, voids are filled with Ag atoms and transformed into metal grains. The estimates [10, 11] showed that the mean grain radius is about 3 nm. Let the voids in quartz glass be spherical. In accordance with (4), the q value is determined by either the volume V of a void with radius a or their concentration N. At large V (i.e., at $a \sim \lambda$), light scattering should be observed. However, quartz glass does not scatter even UV light; therefore, the inequality $a \ll \lambda$ should be satisfied. Let us assume that the Ag grain radius coincides with the void radius during implantation, i.e., $a \approx 3$ nm. Then, the average void volume $V = 4\pi a^3/3 \approx 10^{-19}$ cm^3. Using (4), we find that the void concentration $N = 1.68 \times 10^{18}$ cm^{-3} at $q = 0.168$. Furthermore, assuming some self-organization in the quartz glass structure, we can determine the average distance S between the centers of neighboring spherical voids: $S = N^{-1/3} \approx 1.2 \times 10^{-6}$ cm = 12 nm. Hence, neighboring voids are separated by gaps of about 6 nm.

The estimated void sizes should correspond to the real quartz glass structure. The data on possible void sizes, which were obtained by studying the solubility of different gases in quartz glass, were reported in [16]. According to these data, the sizes (diameters) are within ≈0.2–1.0 nm, i.e., almost an order of magni-

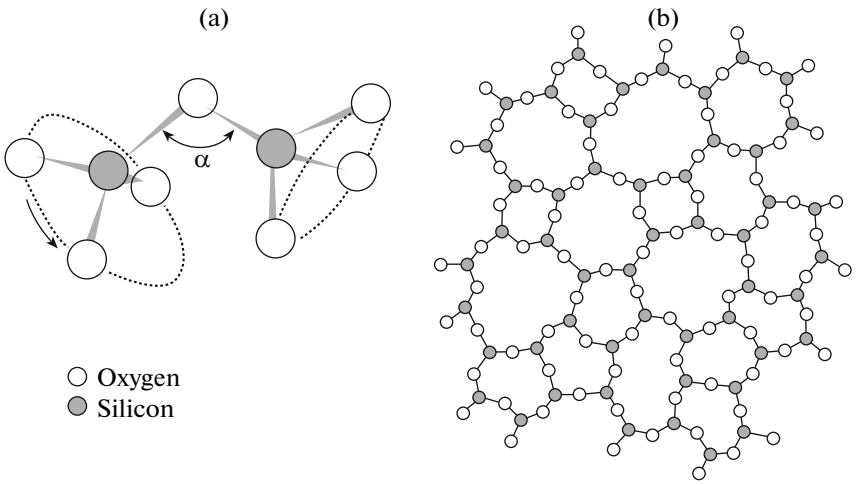

Fig. 4. Quartz glass structural elements and network: (a) two silicon–oxygen tetrahedra and (b) the projection of a continuous random quartz glass network structure onto a plane.

tude smaller than our estimate. The voids are formed by spatial rings of SiO_4 tetrahedra. The spread in size is determined by the number of tetrahedra in the ring (Fig. 4b). The methods of computer simulation of the quartz glass structure predict the existence of large voids, formed by seven- and eight-membered rings. The fraction of these voids is about 28%. The studies devoted to the diffusion of O_2 molecules through *a*-SiO_2 film growing on silicon were also noted in [16]. It was suggested in these studies that defects are present in the form of channel-like voids formed by large (seven- and eight-membered) rings and oriented perpendicularly to the film boundaries. It is suggested that channel-like voids are also characteristic of bulk quartz glass.

The rare and deep pits observed on clean quartz glass surface (Fig. 2c) could be related to the above-mentioned channel-like voids, but their diameters are too large (≈50–80 nm) for this type of identification. Therefore, the origin of these pits and their role in the silver implantation into quartz glass remains open.

The inconsistency between our estimate of the void size and the data in the literature suggests that the silver implantation can be accompanied by the diffusive coagulation of voids, leading to their significant growth. The diffusion can stimulate the difference in the local surface temperatures in the sites of the location of molten Ag particles and in the gaps between them (based on the assumption that Ag particles are crystalline, the temperature during their melting should remain constant and close to the Ag melting temperature). At the same time, the temperature in the gaps between particles can be much higher. The temperature gradient can facilitate the diffusion of voids in the quartz glass surface layer and their coagulation near Ag particles. The expansion of voids facilitates the formation of Ag particles with radii in several nanometers in them.

Note also that the implantation deforms the quartz glass surface with the formation of a surface relief both in the case of isotropic colloid implantation [10, 11] and in the case of Ag PS implantation considered here (Figs. 2a, 2b). This fact indicates the significant deformation of the quartz glass structural network near the surface as a result of Ag particle implantation. This deformation is apparently accompanied by a break in the oxygen bridges between tetrahedra, which leads to an increase in the void size and the concentration of defects in the structural network of the quartz glass.

In the range of the quartz glass annealing and softening temperatures (1000–1300°C), at which implantation occurs, the most likely defects of the structural network are $Si^{3+}O_{3/2}$, $Si^{2+}O_{2/2}$, and like structural groups, nonsaturated with oxygen. These defects are related to coloring the quartz glass (synthesized under reducing conditions and subjected to subsequent heat treatment) with colloidal copper [16]. In this case, copper impurity can be present in the quartz glass or pass to it from heating and reinforcing elements of the furnace where a heat treatment is performed. The coloring reaction can be written as

$$SiO_{3/2}O^-Cu^+ + Si^{3+}O_{3/2} \underset{>1400^\circ C}{\overset{<1400^\circ C}{\rightleftharpoons}} 2SiO_{4/2} + Cu^0. \quad (6)$$

This reaction is reversible: when quartz glass is heated to $T \approx 1800$°C and rapidly cooled, it becomes colorless due to the shift of reaction (6) to the left. Apparently, a similar chemical process occurs for Ag^+ ions. Note also that silver is implanted into a thin (~100 nm [10, 11]) quartz surface layer. The surface may contain rough defects, as is evidenced by the presence of large pits on clean quartz glass surface (Fig. 2c). The reaction of type (6) is indirectly evi-

denced by the formation of craters in surface protrusions (Fig. 2b), which can be formed as follows. Molten silver dissolves oxygen well, which is then intensively released upon rapid silver solidification [20]. After implantation, the sample was rapidly extracted from the CO_2-laser beam and cooled to $T \approx 100°C$ for about 1 min in air.

Thus, along with filling voids by Ag particles due to the thermal diffusion of electrons and Ag^+ ions, one should also take into account the possibility of reactions of type (6), which are related to the defects of glass structural network and lead to the formation of neutral Ag atoms.

CONCLUSIONS

The thermally induced implantation of metal particles into quartz glass by a CO_2-laser beam has some advantages in comparison with the potential possibility of implanting by heating a sample in a furnace. First, at the quartz glass absorption coefficient $\alpha \approx 400\ cm^{-1}$ for $\lambda = 10.6\ \mu m$ and beam power $P \approx 20$–$20\ W$, a quartz glass layer with a thickness of $\sim\alpha^{-1}$ is rapidly heated to a temperature above 1000°C. The temperature reaches a maximum in the beam penetration region rather than throughout the entire sample volume. The temperature gradients are directed both into the quartz glass bulk and in the radial directions with respect to the beam axis. Heating occurs in a much more pure atmosphere because there are no impurities released from the furnace heating and reinforcing elements.

The necessary condition for implanting an Ag film is its small thickness (<10 nm) and island structure. It is shown in this study that, using a composite photosensitive AgCl–Ag film, one can implant a periodic structure formed by small silver particles into quartz. These structures are similar to diffraction gratings with $d < \lambda$ and can be used to introduce directed modes into quartz. They are also of interest for studying nonlinear optical effects and Raman scattering from monolayers of adsorbed organic molecules. Other implantation methods listed in Introduction are more difficult to implement and do not make it possible to implant structures with a specified silver particle distribution into quartz glass.

REFERENCES

1. R. A. Ganeev, A. I. Ryasnyanskiĭ, A. L. Stepanov, M. K. Kodirov, and T. Usmanov, Opt. Spektrosk. **95** (6), 1034 (2003) [Opt. Spectrosc. **95**, 967 (2003)].
2. U. Kreibig and M. Vollmer, *Optical Properties of Metal Clusters* (Springer, Berlin, 1995).
3. H. Hovel, S. Fritz, A. Hilder, U. Kreibig, and M. Vollmer, Phys. Rev. B **48**, 18 178 (1993).
4. M. Antonello, G. W. Arnold, G. Battaglin, R. Bertoncello, E. Cattaruzza, P. Colombo, G. Mattei, P. Mazzoldi, and F. Trivillin, J. Mater. Chem. **8**, 457 (1998).
5. L. Armelao, R. Bertoncello, E. Cattaruzza, S. Gialanella, S. Gross, G. Mattei, P. Mazzoldi, and E. Tondello, J. Mater. Chem. **12**, 2401 (2002).
6. W. Cai, H. Hofmeister, T. Rainer, and W. Chen, J. Nanopart. Res. **3**, 443 (2001).
7. A. L. Stepanov, Rev. Adv. Mater. Sci. **4**, 123 (2003).
8. A. Nahal, H. R. M. Khalesifard, and J. Mostafavi-Amjad, Appl. Phys. B **79**, 513 (2004).
9. M. Sendova, M. Sendova-Vassileva, J. C. Pivin, H. Hjfmeister, K. Coffey, and A. Warren, J. Nanosci. Nanotechnol. **6** (3), 748 (2006).
10. L. A. Ageev, V. K. Miloslavsky, and E. D. Makovetsky, Opt. Spektrosk. **102** (3), 489 (2007) [Opt. Spectrosc. **102**, 442 (2007)].
11. L. A. Ageev, V. K. Miloslavsky, E. D. Makovetsky, K. Beloshenko, and A. V. Stronsky, Funct. Mater. **14** (1), 24 (2007).
12. L. A. Ageev and V. K. Miloslavsky, Opt. Eng. **34** (4), 960 (1995).
13. L. A. Ageev, V. K. Miloslavsky, H. I. Elashhab, and V. B. Blokha, *Training Experiments and Demonstrations in Optics: A Textbook* (KhNU, Kharkov, 2000) [in Russian].
14. V. K. Miloslavsky, *Nonlinear Optics: A Textbook* (KhNU, Kharkov, 2008) [in Russian].
15. P. V. Meĭklyar, *Physical Processes in the Formation of Latent Photographic Images* (Nauka, Moscow, 1972) [in Russian].
16. V. K. Leko and O. V. Mazurin, *Properties of Quartz Glass* (Nauka, Leningrad, 1985) [in Russian].
17. A. Feltz, *Amorphe und Glasartige Anorganische Festörper* (Verlag, Berlin, 1983; Mir, Moscow, 1986).
18. *Theory, Technology, and Equipment of Diffusion Welding*, Ed. by V. A. Bachin (Mashinostroenie, Moscow, 1991) [in Russian].
19. E. M. Voronkova, B. N. Grechushnikov, G. I. Distler, and I. P. Petrov, *Optical Materials for IR Applications* (Nauka, Moscow, 1965) [in Russian].
20. *Properties of Elements: A Handbook*, Ed. by M. E. Drits (Metallurgiya, Moscow, 1985) [in Russian].

Translated by Yu. Sin'kov